A Solanesyl-diphosphate Synthase Localizes in Glycosomes of *Trypanosoma cruzi*[*]

Marcela Ferella[‡§¶‖], Andrea Montalvetti[¶], Peter Rohloff[¶], Kildare Miranda[**], Jianmin Fang[**], Silvia Reina[‡¶], Makoto Kawamukai[‡‡], Jacqueline Búa[‡], Daniel Nilsson[‖], Carlos Pravia[‡], Alejandro Katzin[§§], Maria B. Cassera[§§], Lena Åslund[§], Björn Andersson[‖], Roberto Docampo[¶**1], and Esteban J. Bontempi[‡§‖2]**

From the [‡]Instituto Nacional de Parasitología Dr. M. Fatala Chabén, Av. Paseo Colón 568, Administración Nacional de Laboratorios e Institutos de Salud, Ministerio de Salud, Buenos Aires 1063, Argentina, the [§]Department of Genetics and Pathology, Uppsala University, Uppsala SE751 85, Sweden, the [¶]Department of Pathobiology, University of Illinois at Urbana-Champaign, Urbana 61802, Illinois, the [‖]Center for Genomics and Bioinformatics, Karolinska Institute, Stockholm SE171 77, Sweden, the [**]Center for Tropical and Emerging Global Diseases and Department of Cellular Biology, University of Georgia, Athens, Georgia 30602-2607, the [‡‡]Department of Applied Bioscience and Biotechnology, Faculty of Life and Environmental Science, Shimane University Matsue 690-8540, Japan, and the [§§]Departamento de Parasitologia, Instituto de Ciencias Biomédicas, Universidade de São Paulo, São Paulo 05508-900, Brazil

We report the cloning of a *Trypanosoma cruzi* gene encoding a solanesyl-diphosphate synthase, *TcSPPS*. The amino acid sequence (molecular mass ~ 39 kDa) is homologous to polyprenyl-diphosphate synthases from different organisms, showing the seven conserved motifs and the typical hydrophobic profile. TcSPPS preferred geranylgeranyl diphosphate as the allylic substrate. The final product, as determined by TLC, had nine isoprene units. This suggests that the parasite synthesizes mainly ubiquinone-9 (UQ-9), as described for *Trypanosoma brucei* and *Leishmania major*. In fact, that was the length of the ubiquinone extracted from epimastigotes, as determined by high-performance liquid chromatography. Expression of *TcSPPS* was able to complement an *Escherichia coli ispB* mutant. A punctuated pattern in the cytoplasm of the parasite was detected by immunofluorescence analysis with a specific polyclonal antibody against TcSPPS. An overlapping fluorescence pattern was observed using an antibody directed against the glycosomal marker pyruvate phosphate dikinase, suggesting that this step of the isoprenoid biosynthetic pathway is located in the glycosomes. Co-localization in glycosomes was confirmed by immunogold electron microscopy and subcellular fractionation. Because UQ has a central role in energy production and in reoxidation of reduction equivalents, TcSPPS is promising as a new chemotherapeutic target.

Trypanosoma cruzi is the etiological agent of Chagas disease or American trypanosomiasis, which is the leading cause of cardiac death in endemic areas throughout Latin America. More than 18 million people are infected with the parasite, and some 40 million more are at risk (1).

Chemotherapy of Chagas disease is unsatisfactory because of toxicity and lack of efficacy of existing drugs, and it is important to identify enzymes and metabolic processes in *T. cruzi* that might be potential targets for drug development. One pathway that has been particularly useful for the identification of new targets is the isoprenoid pathway. Enzymes studied so far involved in the synthesis of sterols (2), farnesyl diphosphate (3), and protein prenylation (4) have been reported to be good drug targets against this parasite. The farnesyl-diphosphate synthase, for example, has been demonstrated to be the target of bisphosphonates that have activity *in vitro* and *in vivo* against *T. cruzi* (3, 5–9).

Polyprenyl-diphosphate synthases are responsible for chain elongation in isoprenoid biosynthesis and catalyze the sequential condensation of isopentenyl diphosphate (IPP,[3] C_5) with allylic prenyl diphosphates (10). These condensations are catalyzed by a family of prenyltransferases, which are classified into two groups according to the stereochemistry of the *E* or *Z* double bond that is formed (10). *Z*-Polyprenyl-diphosphate synthases are used for the synthesis of dolichols for *N*-linked glycoprotein biosynthesis, *Z*-polyprenols for peptidoglycan biosynthesis in bacteria, and natural rubber, whereas *E*-poly-

* This work was supported in part by National Institutes of Health Grants AI-68647 and GM-65307 (to R. D.), the Programa de Nanociencia e Nanotecnologia, MCT/CNPq, Brazil (to K. M), the NASA/ChagaSpace network, Consejo Nacional de Investigaciones Científicas y Técnicas (CONICET, Argentina), the Network for Research and Training in Parasitic Diseases at the Southern Cone of Latin America Swedish International Development Agency/Swedish Agency for Research Cooperation and Wallenberg Consortium North, and by the Instituto Nacional de Parasitología Dr. Mario Fatala Chabén, Administración Nacional de Laboratorios e Institutos de Salud, Dr. Carlos G. Malbrán. The costs of publication of this article were defrayed in part by the payment of page charges. This article must therefore be hereby marked "*advertisement*" in accordance with 18 U.S.C. Section 1734 solely to indicate this fact.

The nucleotide sequence(s) reported in this paper has been submitted to the GenBank™/EBI Data Bank with accession number(s) AF282771.

[1] To whom correspondence may be addressed: Center for Tropical and Emerging Global Diseases and Dept. of Cellular Biology, 350 Paul D. Coverdell Center, University of Georgia, Athens, GA 30602-2607. Tel.: 706-542-3310; Fax: 706-583-0181; E-mail: rdocampo@uga.edu.

[2] To whom correspondence may be addressed. Tel.: 54-11-4331-4019; Fax: 54-11-4331-7142; E-mail: ejbon@yahoo.com.

[3] The abbreviations used are: IPP, isopentenyl diphosphate; DMAPP, dimethylallyl diphosphate; GPP, geranyl diphosphate; FPP, farnesyl diphosphate; GGPP, geranylgeranyl diphosphate; UQ, ubiquinone; SPP, solanesyl diphosphate; SPPS, solanesyl-diphosphate synthase; TcSPPS, *T. cruzi* solanesyl-diphosphate synthase; PPDK, pyruvate phosphate dikinase; HMG-CoA, 3-hydroxy-3-methylglutaryl coenzyme A; HPLC, high-performance liquid chromatography; MOPS, 4-morpholinepropanesulfonic acid; RT, reverse transcription; GAPDH, glyceraldehyde-3-phosphate dehydrogenase.

prenyl-diphosphate synthases are used for the synthesis of a vast variety of important natural isoprenoids, such as steroids, cholesterol, sesquiterpenes, heme a, dolichols, farnesylated proteins, carotenoids, diterpenes, geranylgeranylated proteins, chlorophylls, and archaebacterial ether-linked lipids (10). Long *E*-polyprenyl-diphosphate synthases producing compounds with chain lengths from C_{30} to C_{50} are involved in respiratory quinone biosynthesis (10).

So far, only the genes encoding farnesyl diphosphate (FPP) synthases have been studied in trypanosomatids (5, 11). This is despite the presence of ubiquinone 9 (UQ-9), the product of a biosynthetic pathway beginning with the condensation of *p*-hydroxybenzoic acid and solanesyl diphosphate (SPP, C_{45}), in *Leishmania* (12–14), *T. brucei* (15, 16), *Crithida fasciculata* (17), and *Crithidia oncopelti* (18) and the finding that, at least in *L. major* and *T. brucei* (12, 16), labeled precursors (acetate and mevalonate, and mevalonate, respectively) are incorporated into UQ. These results imply the presence of a solanesyl-diphosphate synthase (SPPS) in these parasites.

The localization of the trypanosomatid enzymes involved in isoprenoid metabolism has been little studied, although some of them, like the *T. cruzi* FPP synthase (5), bear predicted targeting signals for the glycosomes. Glycosomes are specialized peroxisomes that, like them, contain several enzymes in pathways of ether lipid synthesis, fatty acid β-oxidation, and peroxide metabolism, and, in addition, contain the Embden-Meyerhof segment of glycolysis (19).

In the present study, we report the cloning, sequencing, and heterologous expression of a *T. cruzi* gene designated *TcSPPS* that encodes a functional SPPS. The expressed *TcSPPS* gene could complement the function of the corresponding polyprenyl-diphosphate synthase of *Escherichia coli*, and the cells produced mainly UQ-9. The kinetic properties of the recombinant TcSPPS were analyzed, and the enzyme was shown to localize in the glycosomes, supporting the role of these organelles in isoprenoid synthesis.

EXPERIMENTAL PROCEDURES

Materials—Newborn calf serum, Dulbecco's phosphate-buffered saline, protease inhibitor mixture, dimethylallyl diphosphate (DMAPP), geranyl diphosphate (GPP), FPP, geranylgeranyl diphosphate (GGPP), and IPP were purchased from Sigma. [4-^{14}C]IPP (57.5 mCi/mmol) was from PerkinElmer Life Sciences. Adsorbosil RP HPTLC plates were from Alltech (Deerfield, IL). Benzonase™ nuclease was from Novagen (Madison, WI). Nickel-nitrilotriacetic acid-agarose was obtained from Qiagen (Valencia, CA). PD-10 desalting column was from Amersham Biosciences. Plasmid and cosmid DNA was obtained using the Wizard miniprep kits (Promega, Madison, WI). PCR products were purified using the Concert kit (Life Technologies, Rockville, MD). Affinity purified *T. cruzi* SPPS antibodies were obtained as described previously (11). Anti *T. brucei* pyruvate phosphate dikinase (PPDK)-producing mouse hybridoma culture supernatant was a gift from Frederique Bringaud (University of Bordeaux, France); rabbit anti-TbgGAPDH antibody was provided by Fred Opperdoes (University of Louvain, Belgium); anti-*T. brucei* vacuolar pyrophosphatase (TbVP1) was a gift from Norbert Bakalara (Ecole Nationale Superiéure de Chimie de Montpellier, France); MitoTracker Red CMXRos, anti-mouse Alexa 488, and anti-rabbit Alexa 546 were from Molecular Probes (Eugene, OR). Co-enzyme Q_{10} was purchased from Sigma. Co-enzyme Q_8 was isolated from *E. coli* by extraction with hexane and further purification by high-performance liquid chromatography (HPLC) as described by Okamoto and co-workers (20). All solvents were HPLC grade.

Culture Methods and Cell Extraction—*T. cruzi* amastigotes and trypomastigotes (Y strain) were obtained from the culture medium of L_6E_9 myoblasts as described previously (21). *T. cruzi* epimastigotes (Y strain) were grown at 28 °C in liver infusion tryptose medium (22) supplemented with 10% newborn calf serum. *T. cruzi* epimastigotes (CL Brener clone) were grown as described before (23).

DNA Sequencing and Bioinformatics—Sequencing grade DNA was obtained using a Qiagen kit. Sequencing was performed on an ABI 377 using a BigDye Terminator Cycle Sequencing Kit (PerkinElmer Life Sciences), or on a MegaBACE 1000 using the DYEnamic ET dye terminator kit (Amersham Biosciences). Vector primers and the following sequencing primers were used: Fwd (antisense), 5′-CACGTGCCACCATGGCAAAC-3′; Fwd2 (antisense), 5′-CAATGCCTTCTGCCATGTC-3′. Chromatograms were analyzed using Bio Edit software (24). Homology searches were performed at the NCBI Blast server (25), and sequences were aligned using ClustalX VI 1.81. The theoretical molecular weight and isoelectric point were obtained from the ExPASy Server (cn.expasy.org). The superimposed hydrophobicity profiles were calculated using the Kyte-Doolittle hydropathy algorithm (26) at bioinformatics.weizmann.ac.il/hydroph. The presence of a signal peptide was assessed by the SignalP 3.0 software (www.cbs.dtu.dk/) (27).

Hybridization to Cosmid Filters—Cosmid filters from a CL Brener cosmid library were used (28). The whole coding sequence of the gene was generated by PCR, purified from agarose gels using DEAE membranes (29), and 30 ng was labeled with [α-^{32}P]dCTP by random priming (Prime a Gene, Promega). Cosmid filters were prehybridized and hybridized as described (28), using a Micro 4 oven (Hybaid, UK). Two of the positive clones (20i8 and 69i5) were further studied.

Hybridization to Pulsed Field Gel Electrophoresis and Northern Filters—Chromosomes from the *T. cruzi* CL Brener clone were separated by pulsed field gel electrophoresis using different running conditions (30) and transferred to nylon filters (kindly provided by Mario Galindo, Instituto de Ciencias Biomédicas, Facultad de Medicina, Universidad de Chile). *Schizosaccharomyces pombe* and *Saccharomyces cerevisiae* chromosomes were used as markers (Bio-Rad). Total RNA from epimastigotes was isolated using an SV Prep Total RNA kit (Sigma), according to the manufacturer's instructions. For Northern blot analysis, epimastigotes total RNA was subjected to electrophoresis in 1% agarose gel containing 1× MOPS buffer and 6.29% (v/v) formaldehyde after boiling for 10 min in 50% (v/v) formamide, 1× MOPS buffer, and 5.9% (v/v) formaldehyde. The RNA was transferred to a Hybond-N filter. A *T. cruzi* probe encoding the 19-kDa cyclophilin, *TcCyP19*, was used as a positive control.

RT-PCR—T. cruzi CL Brener epimastigote mRNA was isolated by using a QuickPrep Micro mRNA kit (GE Healthcare Bio-Sciences), and RT-PCR was performed with the Access RT-PCR System (Promega) using the following primers at 1 μM final concentration: Miniexon (sense), 5′-AACGCTATTATT-GATACAGTTTCTGTACTATATTG-3′, Fwd2 (antisense). As an internal positive control *TcCyP19* was amplified.

Southern Blot Analysis and Genome Organization—T. cruzi CL Brener genomic DNA (3 μg) was digested by NcoI and AatII (Fermentas), separated on a 1% agarose gel and transferred to Hybond-N^+ membrane (Amersham Biosciences). Efficient transfer was confirmed by methylene blue staining (Sigma). Probe generation and target detection was performed using the Gene Images AlkPhos Direct Labeling & Detection system (Amersham Biosciences) following the manufacturer's instructions. Blast searches of the *T. cruzi* genome (www.genedb.org/genedb/tcruzi/) were performed with *TcSPPS* nucleotide sequence. *In silico* restriction analysis was performed at The Sequence Manipulation Suite web site (bioinformatics.org/sms/).

Expression and Purification of TcSPPS from E. coli—For expression in *E. coli*, the entire coding sequence of the *TcSPPS* gene was amplified by PCR using primers (PS5, 5′-CCGGAT-CCATGCTGAAAACAGGCCTTT-3′; PS3, 5′-CCAAGCTT-CATACTTGTCGCGTTAAAA-3′) that introduced BamHI and HindIII restriction sites for convenient cloning into the expression vector pET-$28a^+$ to yield pET-*TcSPPS*. The joining region was sequenced for confirmation. *E. coli* BL21(DE3) bacterial cells transformed with pET-*TcSPPS* were induced, and the recombinant protein was purified by nickel-nitrilotriacetic acid-agarose, following the standard Qiagen procedure. The eluted fraction was desalted with a PD-10 desalting column. Proteins were quantified by the Bradford method (31) with bovine serum albumin as a standard and the absence of protein contaminants was checked by SDS-PAGE.

Measurement of Activity and Product Analysis—Enzyme activity was measured by determination of the amount of [4-^{14}C]IPP incorporated into butanol-extractable polyprenyl diphosphates. Because removal of the polyhistidine tag resulted in complete loss of activity of other prenyltransferases from trypanosomatids (5, 11), this was not done. The standard assay mixture contained, in a total volume of 100 μl, 100 mM Tris-HCl buffer (at physiological pH 7.4), 1 mM $MgCl_2$, 1% (v/v) Triton X-100, 100 μM [4-^{14}C]IPP (1 μCi/μmol), allylic substrate (400 μM DMAPP, 400 μM GPP, 30 μM FPP, or 50 μM GGPP), and 0.5–3 μg of the purified protein. The mixture was incubated at 37 °C for 30 min, and the reaction was stopped by chilling quickly in an ice bath. The reaction products were then extracted with 1 ml of 1-butanol saturated with water. The 1-butanol layer was washed with water saturated with NaCl, and radioactivity in the butanol extract was determined with a liquid scintillation counter. One unit of enzyme activity was defined as the activity required to incorporate 1 nmol of [4-^{14}C]IPP into extracted product in 1 min. To identify the reaction products after the enzymatic reaction, the radioactive prenyl diphosphates in the mixture were hydrolyzed to the corresponding alcohols with potato acid phosphatase as described before (32). The alcohols were extracted with *n*-pentane and analyzed by TLC on a reversed-phase Adsorbosil HPTLC plate with a solvent system of acetone/water (12:1, v/v). The positions of authentic standards were visualized by iodine vapors. The radioactivity was visualized by autoradiography.

Glycosome Enrichment—T. cruzi CL Brener epimastigotes ($\sim 10^9$ cells) were centrifuged for 10 min at 2,000 $\times$ *g*, and washed twice in TEDS buffer (25 mM Tris-HCl, pH 7.4, 1 mM EDTA, 250 mM sucrose, 1 mM dithiothreitol) containing protease inhibitors (P8340, Sigma). After freezing at −80 °C for 20 min and thawing at 37 °C, cells were centrifuged and resuspended in homogenization buffer (250 mM sucrose, 1 mM EDTA, 0.1% v/v ethanol, 5 mM MOPS, pH 7.2, and protease inhibitors). The parasites were grinded in a pre-chilled mortar with 1× wet weight silicon carbide until no intact cells were observed under the light microscope. The lysate was centrifuged at 100 $\times$ *g* for 10 min to remove the silicon carbide, which was washed in homogenization buffer, and both supernatants were combined (Fraction A). A centrifugation at 1,000 $\times$ *g* for 15 min was performed to remove the nuclei, and the supernatant (Fraction B) was centrifuged at 33,000 $\times$ *g* to enrich in glycosomes. The supernatant was Fraction C (cytoplasm) and the pellet (Fraction D) was the glycosomal enriched fraction. The whole procedure was performed twice. Protein concentration of each fractionation step was measured by a colorimetric assay (Protein Assay, Bio-Rad).

Western Blot Analysis—To investigate for protein expression in the different stages, total trypanosome proteins (30 μg of protein/lane) were separated by SDS-polyacrylamide gel (10%) and transferred to nitrocellulose. Membranes were probed with 1:3,000 dilution of a rabbit anti-SPPS and then with horseradish peroxidase-conjugated anti-rabbit IgG antibody (1:10,000). Immunoblots were developed using the ECL™ chemiluminescent detection kit (Amersham Biosciences).

For Western blot analysis of the different subcellular fractions, the blots were sequentially probed with a rabbit anti-TbgGAPDH antibody as a marker for glycosomes at a dilution of 1:3,000, and after a stripping step, with rabbit anti-TcSPPS antibody.

Complementation Analysis—The *TcSPPS* was tested for its capacity to complement the *ispB* gene of *E. coli*. Strain KO229, whose essential *ispB* gene was disrupted and complemented by the *ispB* expression vector pKA3 (spectinomycin-resistant), was subjected to a plasmid-swapping experiment (33). Because the pET construct would not be inducible in strain KO229, the gene was subcloned into pQE30 vector (pQE-*TcSPPS*). After transformation with pQE-*TcSPPS*, the colonies were grown and passaged for several days in LB medium (1% tryptone, 0.5% yeast extract, 1% sodium chloride, pH 7.5) supplemented with ampicillin (to select pQE-*TcSPPS*-carrying colonies) and isopropyl 1-thio-β-D-galactopyranoside (to induce expression of the His_6-TcSPPS fusion protein). Isolated colonies were checked for ampicillin resistance and spectinomycin sensitivity.

Ubiquinone Extraction and Measurement—Ubiquinone was extracted as previously described (34). The crude extract of UQ was analyzed by normal-phase TLC with authentic standard UQ-10. Normal-phase TLC was carried out on a Kieselgel 60 F_{254} plate (Merck) with benzene/acetone (93:7, v/v). The band containing UQ was collected from the TLC plate following UV visualiza-

tion and extracted with chloroform/methanol (1:1, v/v). Samples were dried and re-dissolved in ethanol. The purified UQ was further analyzed by HPLC with ethanol as the solvent.

Fluorescence Microscopy—For co-localization with a glycosomal marker, *T. cruzi* Y strain epimastigotes slides were prepared as previously described (35). Antibody concentrations were as follows: affinity-purified rabbit anti-TcSPPS antibody at 1:4,000; supernatant from an anti-TbPPDK producing mouse hybridoma culture at 1:10; anti-mouse Alexa 488 at 1:1,000; anti-rabbit Alexa 546 at 1:1,000. For co-localization studies with MitoTracker and the vacuolar pyrophosphatase, epimastigotes were fixed for 30 min in 4% paraformaldehyde in 0.1 M cacodylate buffer, washed twice in Dulbecco's phosphate-buffered saline, pH 7.2, adhered to poly-L-lysine-coated coverslips, and permeabilized for 3 min with 0.3% Triton X-100. Cells were blocked for 30 min in 50 mM NH_4Cl and 3% bovine serum albumin in phosphate-buffered saline, pH 8.0, and incubated for 1 h with polyclonal primary antibodies raised against *T. cruzi* SPPS (1:1000), and monoclonal antibodies raised against *T. brucei* VP1 (1:200). For mitochondrial staining, cells were previously incubated for 30 min in culture medium containing 100 nM MitoTracker before fixation. Cells were then washed in 3% bovine serum albumin, incubated with secondary antibodies anti-mouse Alexa 488 (1:1,000), anti-rabbit Alexa 488, and anti-rabbit Alexa 546 (1:1,000) and mounted in prolong Antifade. Cells were observed in a Deltavision fluorescence microscope. Images were recorded with a Photometrics CoolSnap HQ camera and deconvolved for 15 cycles using Softwarx deconvolution software.

Immunogold Electron Microscopy—Immunogold electron microscopy experiments were performed as described previously (35) using the rabbit anti-SPPS antibody (1:100) and a monoclonal antibody against *T. brucei* pyruvate-phosphate dikinase (1:10). After washing, the grids were incubated with 18 nm colloidal gold-AffiniPure-conjugated anti-rabbit IgG (H + L) and 12 nm colloidal gold-conjugated goat anti-mouse IgG (H + L). Images were acquired on a Phillips CM-200 transmission electron microscope operating at 120 kV.

RESULTS

Identification of T. cruzi SPPS—We determined the complete sequence of the *T. cruzi* cDNA clone TENU4155 (accession number AW324852) (36), which showed similarities to polyprenyl synthases. The sequence surrounding the first ATG complied with the published rules for start codons in protozoa (37). To obtain further upstream sequences a cDNA probe was hybridized to high density cosmid filters, and the sequence obtained from two of the positive clones (20i8 and 69i5) with the forward primer displayed a stop codon in the same reading frame as the first putative ATG, confirming the protein coding region. This sequence has been submitted to the GenBank™ under the accession number AF282771.

Translation of the open reading frame of 1092 bp yielded a polypeptide of 363 amino acids with a predicted molecular mass of 39 kDa and an isoelectric point of 6.01. A small residue (Ala) is found at position −5 before the first aspartate-rich motif. This position is diagnostic, determining the final product length (for a review, see Ref. 38). Bulky amino acids do not allow nascent long chains to extend further inside the hydrophobic cavity of the enzyme. A BLAST search of the protein data base showed that the amino acid sequence from *T. cruzi* shared up to 38% identity and up to 61% similarity with other polyprenyl synthases. Considering specifically the human homologue (accession number NP_055132), the identity reached 33%.

The amino acid sequence from the *T. cruzi* enzyme was aligned with other representative polyprenyl synthases (Fig. 1*A*). All the conserved motifs involved in catalysis or binding (regions I–VII) identified in other polyprenyl synthases (39) are present in the *T. cruzi* enzyme. The functional residues conform also several motifs present in databases, pfam00348 among them, related to *trans*-isoprenyl-diphosphate synthases, as well as motif COG0142, IspA, related to farnesyl-diphosphate synthases. Hydrophobicity analysis of the protein showed the characteristic pattern of this family of enzymes (40), consisting of alternating hydrophobic regions, which in Fig. 1*B* is superimposed to the pattern of the human homologue for comparison.

Four features were observed when comparing the putative *T. cruzi* polyprenyl synthase to those from other species: a shorter N terminus, an insertion, a "correct length" and a "correct charge" of the C terminus (Fig. 1*A*). The N-terminal length variation does not seem relevant, because some species also have a longer N terminus (*Homo sapiens*, *Capsicum annum*, and both SPPS from *Arabidopsis thaliana*) (41, 42). The observed 15-amino acid insertion, based on the proposed structure of polyprenyl synthases (40), could be located in loop 2, which seems not to be involved in binding to the substrate. This should minimize the effect of this difference in the overall structure and in the activity. The C terminus length seems to be significant, because it is claimed to form a flexible flap that seals the active site upon substrate binding (40). Regarding the C terminus charge, the majority of these proteins have positive side-chain amino acids in some of the last three positions (40), which is also the case for TcSPPS (Fig. 1*A*).

The genes encoding TcSPPS were located in homologue chromosomes of sizes 800 and 1100 kb, as assessed by hybridization to pulsed field gel electrophoresis membranes (data not shown). By analysis of the codon usage (bioinformatics.org/sms/) a preference for A- and T-ending codons was detected. The gene could then be assigned to groups TC2 or TC3, conformed by genes using non-optimal codons, which are not highly expressed (43).

Southern Blot and Genome Analysis—Four sequences with homology with *TcSPPS* were present in the contigs generated by the Genome Project. Three of the contigs contained incomplete genes. Two of them were identical in the overlap, had some differences in comparison to the whole gene, and could represent one allele. The third contig was a mix of the two alleles and could arise from an assembly problem. The fourth and longest contig (GenBank™ accession number AAHK01002353) contained within its 6233 bp the complete *TcSPPS* coding region (locus tag Tc00.1047053509445.30), with identical sequence to TENU4155. The size of the fragments generated by complete digestion of total genomic DNA with NcoI (bands of ~1000 and 2500 bp, Fig. 2) agreed with the theoretical restriction map of this contig (data not shown). The

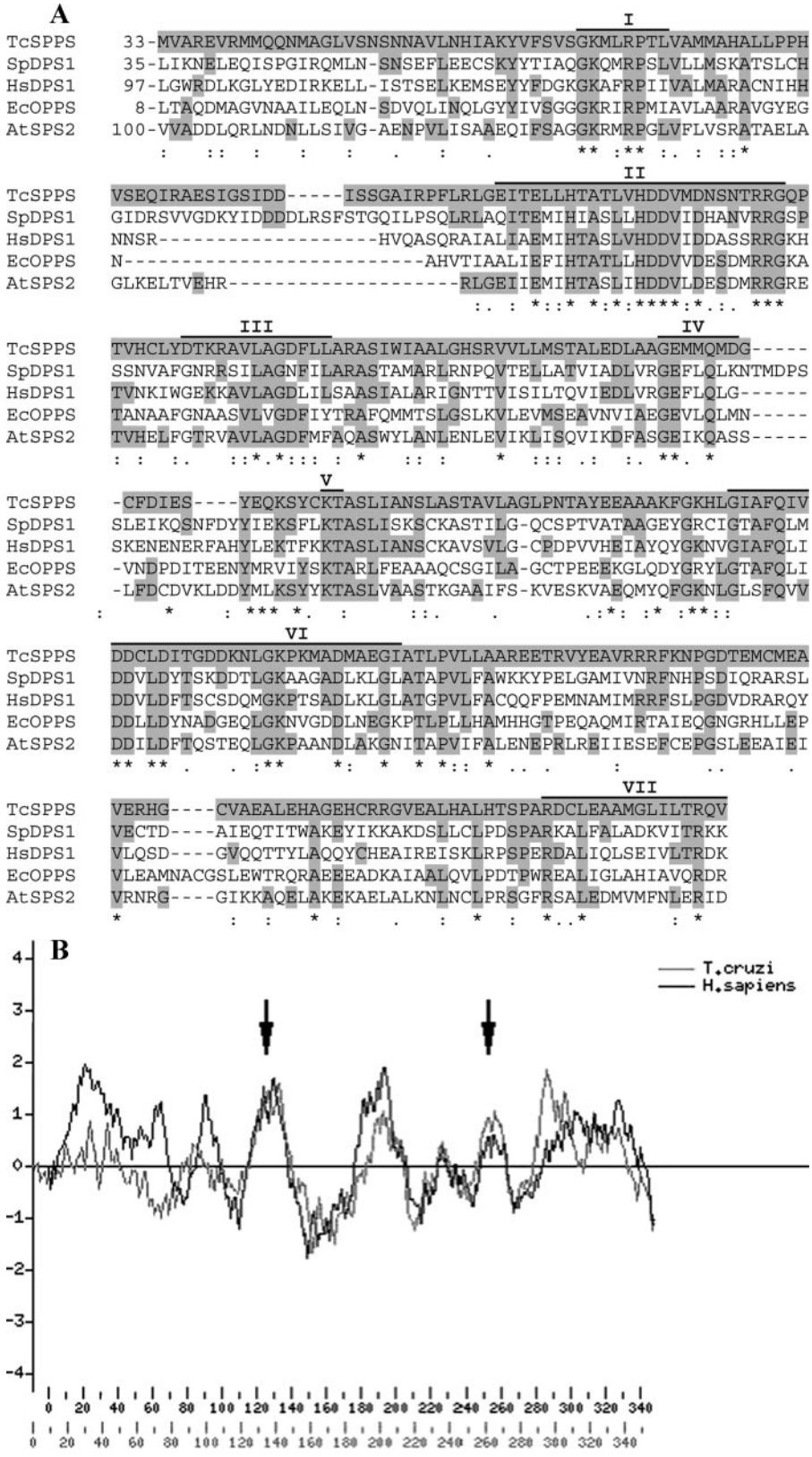

FIGURE 1. **Multialignment of prenyl-diphosphate synthases (*A*) and comparison of the hydrophilicity of human and parasite enzymes (*B*).** *A*, the activity of these proteins has been experimentally demonstrated, although catalytic subunits SpDPS1 and HsDPS1 are not functional alone (62, 63). *Shaded areas* represent amino acids identical to those in TcSPPS. Identical or conserved amino acids in a given position are denoted by *asterisks* and *colons*, respectively. *SpDPS1*, *S. pombe* decaprenyl-diphosphate synthase subunit 1 (O43091); *HsDPS1*, *H. sapiens* decaprenyl-diphosphate synthase subunit 1 (AB210838); *EcOPPS*, *E. coli* octaprenyl-diphosphate synthase (P19641); *AtSPS2*, *A. thaliana* solanesyl-diphosphate synthase 2 (AB188498). The *numbers* at the beginning of the sequences represent the variation in length at the N-terminal end. The seven conserved motifs for *E*-prenyltransferases are in *Roman numerals*. *B*, calculation of hydrophilicity was made using the Kyte-Doolittle method over a window length of 19. Only the homologous regions of both proteins were included. *Arrows* signal the first (FARM) and second (SARM) aspartate-rich motif regions.

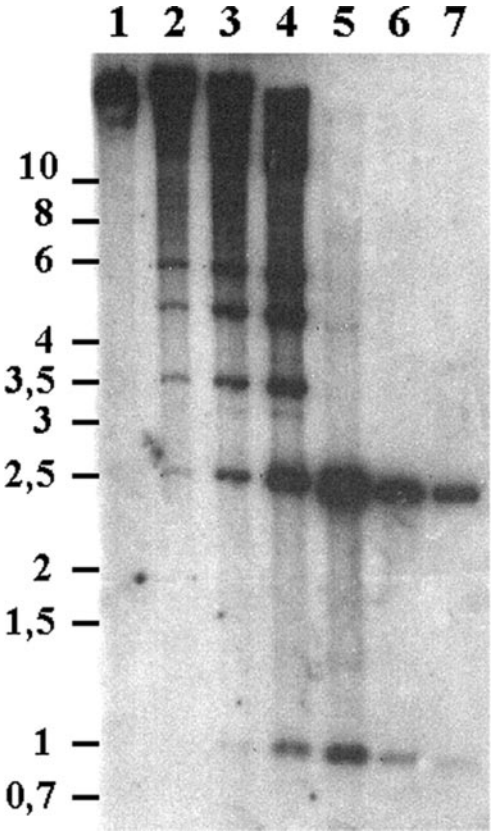

FIGURE 2. **Determination of TcSPPS gene copy number.** Southern blot analysis of NcoI digestion of CL Brener clone genomic DNA. Digestion times were as follows: *Lane 1*, starting material; *2*, 10 min; *3*, 45 min; *4*, 90 min; *5*, 3 h; *6*, 6 h; *7*, overnight (16–18 h). Only two expected fragments were identified by hybridization, showing a single copy gene. Molecular weight markers are indicated on the *left* in kilobases.

same was observed with the AatII digestion pattern (band of ~1000 bp, data not shown). These experiments support the idea that *TcSPPS* is a single copy gene.

Ubiquinone Detection in Complemented E. coli and in T. cruzi Epimastigotes—E. coli has an octaprenyl-diphosphate synthase (44). To test whether the final product of TcSPPS, UQ-9, was able to replace the essential functions of UQ-8, a plasmid-swapping test was carried out using the insertion mutant strain KO229. Several colonies that were ampicillin-resistant (carrying the *TcSPPS*-expressing plasmid) and sensitive to spectinomycin (free of the *ispB*-expressing plasmid) were obtained, suggesting that TcSPPS was fully functional in bacteria. When the UQ of complemented colonies were isolated and their length determined, UQ-9 was the main product detected (Fig. 3*a*). This is in contrast to KO229 harboring pKA3, which produced mainly UQ-8 (Fig. 3*b*). To establish the length of the native molecule in the parasite, UQ was extracted from 1 g of *T. cruzi* epimastigotes and run in HPLC (Fig. 3*c*). The peak corresponded to UQ-9, as reported for other trypanosomatids (12–15).

Functional Analysis of the Candidate Long-chain Prenyl-diphosphate Synthase—For functional analysis, the protein was heterologously expressed in *E. coli* cells as a fusion protein with an N-terminal polyhistidine tag and purified by affinity chromatography (Fig. 4*A*). The purified protein runs close to its predicted molecular mass.

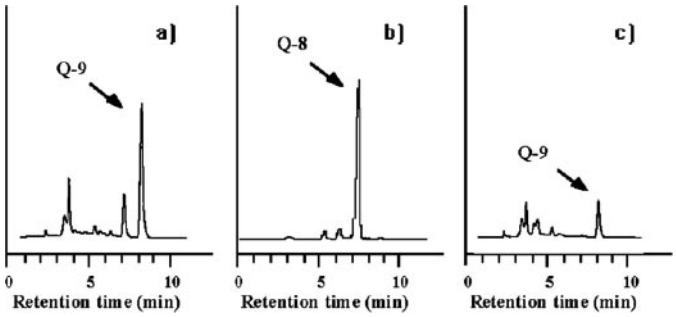

FIGURE 3. **Determination of UQ by HPLC.** *a*, *E. coli* insertion mutant strain KO229 complemented by pQE-TcSPPS recombinant plasmid; *b*, KO229 harboring its essential plasmid pKA3; *c*, *T. cruzi* CL Brener clone epimastigotes.

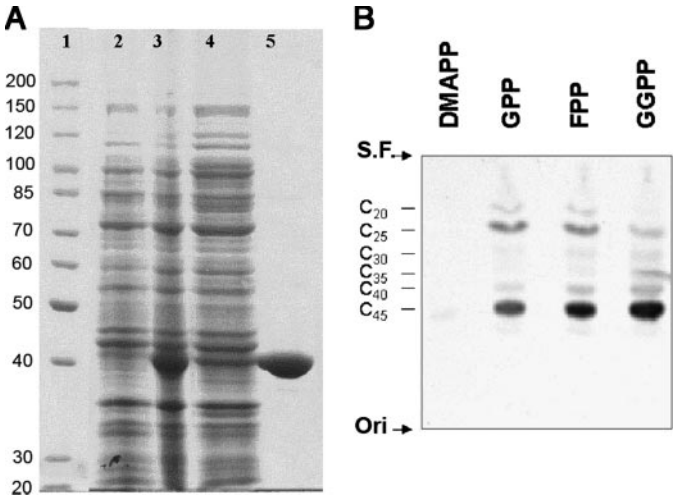

FIGURE 4. **Expression and purification of TcSPPS (*A*) and TLC autoradiograms of prenyl alcohols obtained by enzymatic hydrolysis of the products formed by TcSPPS (*B*).** *A*, recombinant *E. coli* BL21(DE3) (non-induced, *lane 2*) was induced with 0.5 mM isopropyl 1-thio-β-D-galactopyranoside for 3 h at 30 °C (*lane 3*). After sonication the supernatant (*lane 4*) was purified by His tag affinity chromatography (*lane 5*). TcSPPS displayed the expected molecular weight, as evaluated with the protein ladder 10–200 kDa (MBI Fermentas, *lane 1*). *B*, the products obtained from incubation of 100 μM [4-^{14}C]IPP (10 μCi/μmol) and 10 μM DMAPP, GPP, FPP, or GGPP were analyzed by reversed-phase HPTLC as described under "Experimental Procedures." *Ori.*, origin; *S.F.*, solvent front.

The enzymatic activity assay was performed in the presence of different concentrations of Mg^{2+} and Mn^{2+}, to determine their effect on the TcSPPS when the allylic substrate was GGPP. Mg^{2+} and Mn^{2+} were added to the reaction mixture at concentrations between 0.5 and 20 mM. As shown in Table 1, optimal levels of activity were obtained by the addition of 0.5–1 mM Mg^{2+}. The addition of 10 mM EDTA abolished SPPS activity. Enzymatic activity was not detected when the divalent cation was Mn^{2+}. The *T. cruzi* enzyme activity was also assayed between 0.5 and 5% (v/v) Triton X-100. Maximum activity was observed at 1% (v/v) Triton X-100 (using DMAPP, FPP, GPP, or GGPP as primer) (data not shown).

Four kinds of allylic diphosphates were tested as a primer substrate with [4-^{14}C]IPP as described under "Experimental Procedures." The enzyme utilized the four allylic diphosphates as a primer substrate, however, the enzymatic activity using DMAPP as substrate was one order of magnitude lower than the enzymatic activity using FPP, GPP, or GGPP (Table 2). The reaction products were dephosphorylated and then analyzed by

TABLE 1

Effect of divalent cations on TcSPPS

SPPS activity was measured in the presence of the different concentrations of $MgCl_2$ indicated in a reaction medium containing 100 mM Tris-HCl buffer (pH 7.4), 1% (v/v) Triton X-100, 100 μM [4-^{14}C]IPP (1 μCi/ μmol), 50 μM GGPP, and 0.5 μg of recombinant protein (final volume of 100 μl). Reactions were incubated for 30 min at 37 °C and stopped by chilling in an ice bath. The radioactive prenyl products were then extracted with 1-butanol as described under "Experimental Procedures." No activity was detected in the absence of $MgCl_2$ or presence of 10 mM EDTA. Values shown are means ± S.D. of two experiments in duplicate.

$MgCl_2$	SPPS activity
mM	*nmol/min/mg*
0	0
0.5	116.75 ± 0.33
1	121.99 ± 15.78
2	107.53 ± 5.71
5	76.72 ± 12.36
10	47.32 ± 2.56

TABLE 2

Allylic substrate specificity of TcSPPS

SPPS activity was measured in the presence of the different allylic substrates (400 μM DMAPP, 400 μM GPP, 30 μM FPP, 50 μM GGPP) in a reaction medium containing 100 mM Tris-HCl buffer (pH 7.4), 1 mM $MgCl_2$, 1% (v/v) Triton X-100, 100 μM [4-^{14}C]IPP (1 μCi/ μmol), and 0.5–3 μg of the purified protein (final volume of 100 μl). Reactions were incubated for 30 min at 37 °C and stopped by chilling in an ice bath. The radioactive prenyl products were then extracted with 1-butanol as described under "Experimental Procedures." Values shown are means ± S.D. of three experiments in duplicate. A lower activity of the enzyme as compared with that measured in Table 1 indicates a lower amount of active protein per milligram of protein.

Allylic substrate	SPP synthase activity
	nmol/min/mg
DMAPP	3.91 ± 0.07
GPP	34.35 ± 2.29
FPP	17.99 ± 2.09
GGPP	64.34 ± 13.03

TABLE 3

Kinetic parameters of TcSPPS

The kinetic parameters of TcSPPS were determined at 37 °C for 30 min, as described under "Experimental Procedures." The k_{cat} value was defined by units of nanomoles of IPP converted into products per 1 nmol of dimer enzyme per second. Values shown are means ± S.D. of three experiments in duplicate.

Substrate	K_m	k_{cat}	k_{cat}/K_m
	μM	s^{-1}	$s^{-1}\cdot nM^{-1}$
GPP	54.83 ± 5.92	0.065 ± 0.020	1.19
FPP	4.59 ± 0.48	0.032 ± 0.004	7.01
GGPP	7.07 ± 1.08	0.087 ± 0.007	12.35
IPP (400 μM GPP)	19.18 ± 1.16	0.131 ± 0.026	6.85
IPP (30 μM FPP)	30.67 ± 8.44	0.043 ± 0.007	1.40
IPP (50 μM GGPP)	24.33 ± 5.45	0.217 ± 0.032	8.93

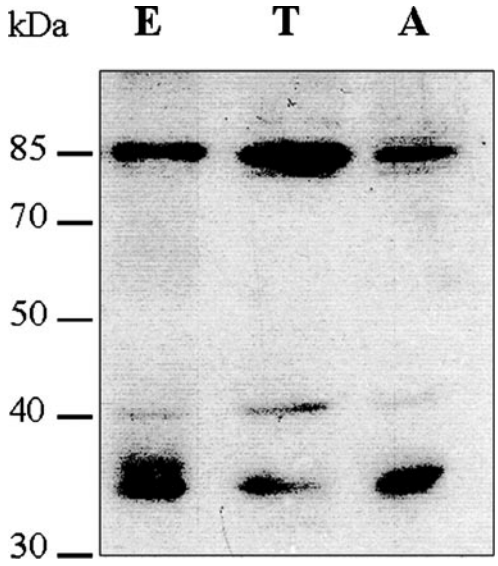

FIGURE 5. **Immunoblot analysis with antibodies against *T. cruzi* SPPS.** Detection of SPPS by immunoblotting using affinity-purified polyclonal antibody against SPPS. Epimastigote (*E*), trypomastigote (*T*), and amastigote (*A*) protein (Y strain, 30 μg/lane) were separated by SDS-PAGE and transferred to a polyvinylidene difluoride membrane.

reversed-phase TLC. When either FPP, GPP, or GGPP was used as the primer substrate, solanesol (C_{45}) was predominantly detected by TLC analysis indicating that the protein generated solanesyl diphosphate (C_{45}) as the major product (Fig. 4*B*). When the primer substrate was DMAPP the labeled products were almost undetectable by TLC.

Kinetic Analysis—Standard procedures were used to determine kinetic parameters. K_m and V_{max} values were obtained by a non-linear regression fit of the data to the Michaelis-Menten equation (SigmaPlot 2000 for Windows), and the results are summarized in Table 3. TcSPPS showed a similar K_m value for FPP and GGPP, however the K_m value for GPP was 7.7-fold higher than that for GGPP. Moreover, the k_{cat} value for GGPP was 2.7-fold higher than that for FPP and slightly higher than that for GPP. Consequently the k_{cat}/K_m value for GGPP was 1.8-fold higher than that for FPP and 10.4-fold higher than that for GPP, indicating that TcSPPS prefers GGPP to FPP or GPP. Moreover, TcSPPS showed a similar K_m value for IPP when the allylic substrate was FPP, GPP, or GGPP. However, when GGPP was used as primer substrate, the enzyme showed a 1.6-fold higher k_{cat} value for IPP than that for IPP with GPP, and a 5.0-fold higher than that for IPP with FPP. Consequently, the k_{cat}/K_m values for IPP with GGPP or GPP were similar, although the k_{cat}/K_m value for IPP with GGPP was 6.3-fold higher than that for IPP with FPP. These results suggest the preference of TcSPPS for GGPP over FPP or GPP.

Presence of mRNA and Protein in T. cruzi—Several assays were used in an attempt to establish the presence of the specific mRNA in CL Brener clone epimastigotes. Neither Northern blot analysis nor RT-PCR amplification allowed the detection of even a negligible amount of mRNA. On the other hand, the mRNA for the positive control used (*TcCyP19* gene) was detected in the Northern and RT-PCR assays. A search was then done on an expressed sequence tag clusters data base (*Tcruzi*DB Version 4.1). A cluster (99127) composed of one read (TcEST_NCBI_AW324852.1) was identified. Its sequence (316 bp) was identical to the 3′-end of the original expressed sequence tag clone, TENU4155 (1262 bp).

Immunoblot analysis with affinity-purified antibody against TcSPPS showed a band of ~36–37 kDa present in all developmental stages of the Y strain (Fig. 5). The antibody also recognized a 85-kDa band in all three stages and more weakly a 40-kDa band. These proteins might share a few epitopes with SPPS in the motif regions.

To further characterize the anti-TcSPPS cross-reaction to other proteins in the parasite, we performed subcellular fractionation experiments to enrich for glycosomes. Fraction D, enriched for glycosomes, showed the strongest reaction by Western blot analysis with antibodies against TcSPPS (Fig. 6*A*) and TbgGAPDH, a glycosomal marker (Fig. 6*B*). In this enrichment experiment, the 40- and 85-kDa bands were not detected in

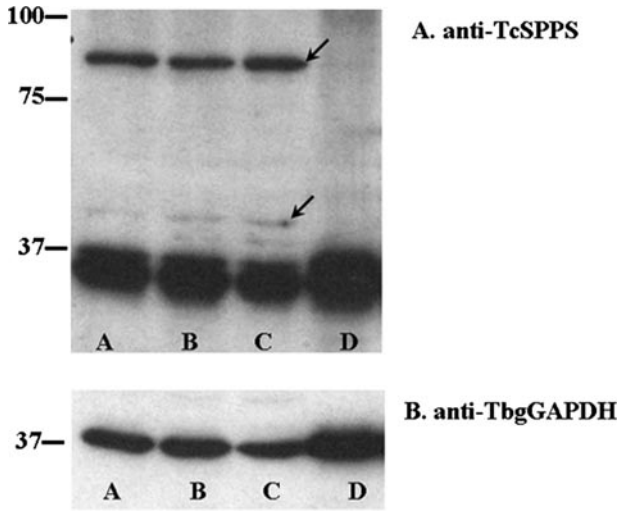

FIGURE 6. **Western blot analysis of glycosome enrichment fractions.** Immunoblots of the fractions (*lanes A–D*) using anti-TcSPPS (*A*) or anti-TbgGAPDH (*B*). The 40- and 85-kDa proteins (*arrows*), detected by anti-TcSPPS, are only detected in the total and cytoplasmic fractions (*lanes A–C*) but not in the glycosome-enriched fraction (*lane D*). Molecular mass markers in kilodaltons are represented in both blots on the *left side*.

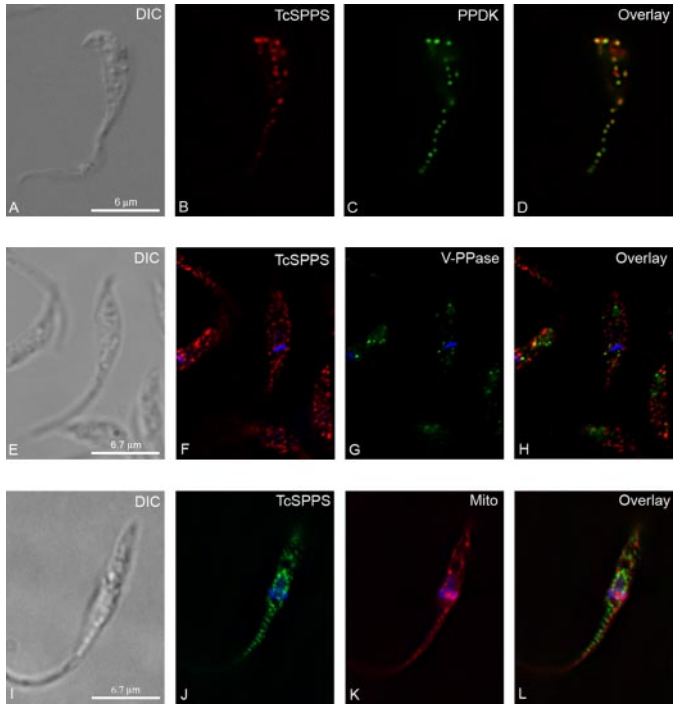

FIGURE 7. **TcSPPS co-localizes with TcPPDK in glycosomes and does not co-localize with acidocalcisome and mitochondrial markers.** Y strain epimastigotes were fixed and stained with anti-TcSPPS antibody (*B*, *F*, and *J*), anti-PPDK antibody (*PPDK*, *C*), anti-vacuolar pyrophosphatase antibody (*V-PPase*, *G*), and MitoTracker (*Mito*, *K*). *DIC* (*A*, *E*, and *I*) and *Overlay* (*D*, *H*, and *L*) images are also shown. *Scale bars* are indicated in *A*, *E*, and *I*.

the pellet fraction (*fraction D*), which was enriched in glycosomes, but were present in the previous steps of the fractionation (*fractions A–C*) (Fig. 6*A*). These bands could be soluble proteins, probably cytoplasmic, that did not localize in glycosomes.

The localization of TcSPPS was further investigated. It is worth mentioning that no import signals (either to endoplasmic reticulum or to glycosomes) were detected. Immunofluorescence microscopy of *T. cruzi* epimastigotes showed co-localization in glycosomes of TcSPPS (Fig. 7*B*) with pyruvate phosphate dikinase (Fig. 7*C*), a known marker of glycosomes (45), as detected with monoclonal antibodies prepared against the recombinant TbPPDK. TcSPPS (Fig. 7*F*) did not co-localize with markers for acidocalcisomes (vacuolar pyrophosphatase) (Fig. 7*G*) or with mitochondrial markers (MitoTracker; Fig. 7, *J* and *K*).

Immunogold electron microscopy confirmed the co-localization of TcSPPS (Fig. 8, *A–C*, 18 nm gold particles) with pyruvate phosphate dikinase (Fig. 8, *A–C*, 12 nm gold particles). The density of TcSPPS gold particles in the glycosomes was significantly higher than in other compartments (Fig. 8*D*). No background staining was observed when secondary antibodies were used alone in immunofluorescence or immunogold electron microscopy assays (data not shown).

DISCUSSION

We report here the functional characteristics of the solanesyl-diphosphate synthase of *T. cruzi* (TcSPPS). Heterologous expression of the *TcSPPS* gene in *E. coli* resulted in the production of a recombinant enzyme that was similar to other SPPSs with respect to its Mg^{2+} requirement but differed in having GGPP as preferred substrate. TcSPPS could complement the function of the corresponding polyprenyl-diphosphate synthase of *E. coli*, and the cells produced mainly UQ-9. The enzyme was shown to localize in the glycosomes, supporting the role of these organelles in isoprenoid synthesis. It is interesting to note that the protein carried neither a PTS1 nor a PTS2 signal, arguing for an alternative import mechanism (for a review, see Ref. 46). This is the first report of a gene encoding a functional SPPS in a trypanosomatid and on its localization in the glycosomes.

Peroxisomes harbor a number of enzymes involved in the isoprenoid pathway. They have been shown to contain acetoacetyl-CoA thiolase (47), 3-hydroxy-3-methylglutaryl (HMG)-CoA synthase (48), HMG-CoA reductase (49), mevalonate kinase (50), and FPPS (51). In addition, they also have a *trans*-prenyltransferase responsible for the generation of SPP and a nonaprenyl-4-hydroxybenzoate transferase involved in the first step of UQ-9 synthesis (52). The soluble HMG-CoA reductase from *T. cruzi* epimastigotes was initially shown to be associated with the glycosomes of this trypanosomatid (53). However, more recent immunogold labeling studies using ultrathin sections of *T. cruzi* epimastigotes and polyclonal/monoclonal antibodies against *T. cruzi* recombinant HMG-CoA reductase and digitonin solubilization experiments suggested that the enzyme is predominantly located inside the mitochondrial matrix (54). Our results indicate that SPPS is located in the glycosomes of *T. cruzi*. Because this enzyme catalyzes a PP_i-producing reaction, the presence in glycosomes of the PP_i-consuming pyruvate phosphate dikinase would make this reaction thermodynamically possible (55, 56).

TcSPPS prefers GGPP over GPP and FPP as substrate. This is in contrast to rat *trans*-prenyltransferase that prefers GPP and IPP as substrates (57). As occurs with the rat enzyme (57), TcSPPS poorly utilized DMAPP. In fact, most SPPSs characterized to date (for example, the ones obtained from rat liver, spinach leaves, and *Micrococcus lysodeikticus*) (57–59) prefer GPP as allylic substrate, so TcSPPS together with *A. thaliana* SPPS1 are the only ones to preferentially use GGPP (42).

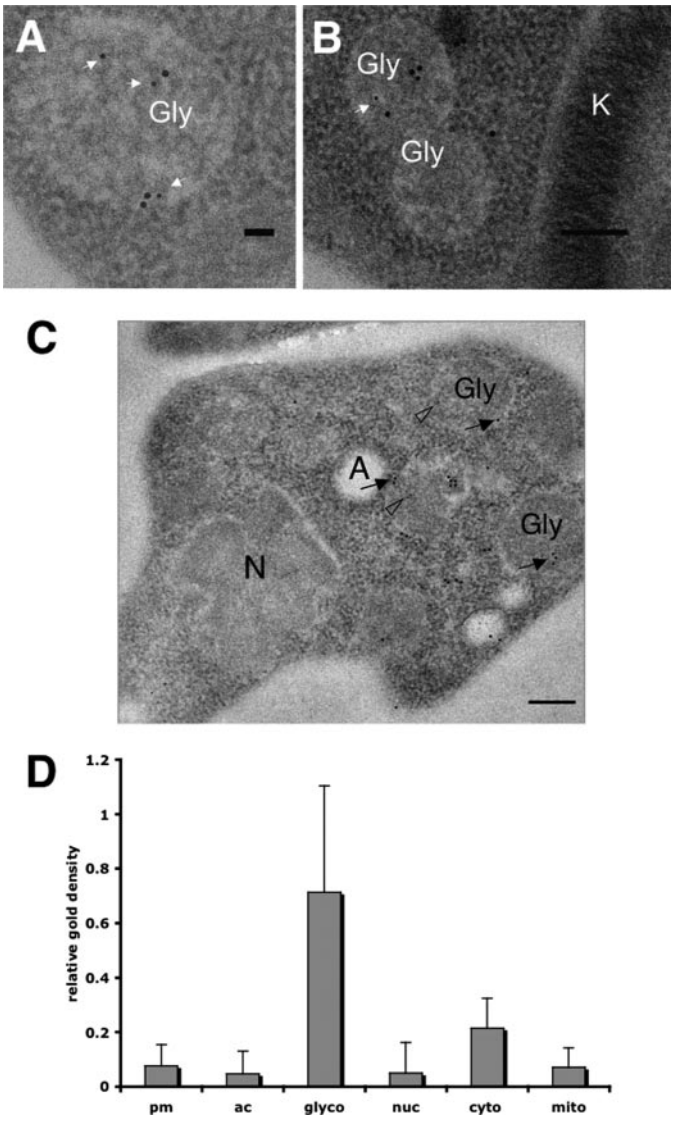

FIGURE 8. **Immunogold electron microscopy showing co-localization of TcSPPS (18 nm gold particles) with TcPPDK (12 nm gold particles).** *A* and *B*, high magnification views showing co-localization to glycosomes. 12 nm gold particles are shown with *white arrows*. *C*, lower magnification view showing the relative specificity of the signal to the glycosomes. *Open arrowheads* indicate TcPPDK signal, and *black arrows* indicate TcSPPS signal. Labeled structures are glycosomes (*Gly*), kinetoplast (*K*), nucleus (*N*), and acidocalcisome (*A*). *Bars*: 0.05 μm (*A*) and 0.1 μm (*B* and *C*). *D*, density histogram representing the relative density distribution of TcSPPS gold particles in five randomly selected thin sections ($\pm$S.D.) by organellar subcompartments: plasma membrane (*pm*), acidocalcisome (*ac*), glycosome (*glyco*), nucleus (*nuc*), cytoplasm (*cyto*), and mitochondrion (*mito*). The difference between TcSPPS density in the glycosome and the next most dense compartment (cytoplasm) was statistically significant ($p < 0.05$) using Student's *t* test.

We succeeded in complementing *E. coli* deficient in polyprenyl-diphosphate synthase. A number of genes encoding polyprenyl-diphosphate synthases from bacteria have been successfully expressed in these *E. coli* mutants (33, 60). The TcSPPS protein is assumed to work as a homodimer, because it is functional without any other genes, unlike the case of *Bacillus subtilis* heptaprenyl-diphosphate synthase (heterodimer) (61), fission yeast decaprenyl-diphosphate synthase (62), mouse solanesyl-diphosphate synthase (63), and human decaprenyl-diphosphate synthase (heterotetramers) (63).

Ubiquinone is synthesized *de novo* in both prokaryotes and eukaryotes. The two parts of the molecule, the benzoquinone ring and the isoprene chain, are synthesized independently and assembled in a reaction catalyzed by a prenyl-4-hydroxybenzoate transferase (64). 4-Hydroxybenzoate originates from tyrosine or phenylalanine in eukaryotes or from acetate through the shikimate pathway in most prokaryotes (65). In trypanosomatids, ubiquinone biosynthesis was investigated in *L. major* and *T. brucei* (12, 16) where it was found that the isoprenoid portion of the molecule is synthesized by the mevalonate pathway (both parasites) and that the ring is synthesized from acetate or aromatic amino acids (*Leishmania*).

Regarding *T. cruzi* UQ chain length, it seems clear, from our *in vitro* (TLC experiment with the purified enzyme in the presence of different substrates) and *in vivo* (HPLC of native UQ) results, that epimastigotes synthesize and retain mainly UQ-9 in their membranes. Valuable functions, even non-traditional ones (66), have been ascribed to this molecule, granting further studies on the importance of the TcSPPS as a new chemotherapeutic target.

Bisphosphonates have been shown to have activity *in vitro* and *in vivo* against *T. cruzi* (1). Some of these compounds (nitrogen-containing bisphosphonates) target the farnesyl-diphosphate synthase (5). However, bisphosphonates can also inhibit other prenyltransferases, and it is expected that bisphosphonates with long side chains, which are known to be potent inhibitors of the intracellular form of *T. cruzi* (67), could target prenyltransferases like TcSPPS.

Acknowledgments—We thank Norbert Bakalara, Frederique Bringaud, and Fred Opperdoes for antibodies, Octavio Fusco for performing the DNA sequencing, Cristina Maidana and Linda Brown for growing the T. cruzi epimastigotes, and Pablo Fazio and Marta Lauricella for technical help.

REFERENCES

1. Urbina, J. A., and Docampo, R. (2003) *Trends Parasitol.* **19,** 495–501
2. Urbina, J. A. (2002) *Curr. Pharm. Des.* **8,** 287–295
3. Docampo, R., and Moreno, S. N. J. (2001) *Curr. Drug Targets Infect. Disord.* **1,** 51–61
4. Gelb, M. H., Van Voorhis, W. C., Buckner, F. S., Yokoyama, K., Eastman, R., Carpenter, E. P., Panethymitaki, C., Brown, K. A., and Smith, D. F. (2003) *Mol. Biochem. Parasitol.* **126,** 155–163
5. Montalvetti, A., Bailey, B. N., Martin, M. B., Severin, G. W., Oldfield, E., and Docampo, R. (2001) *J. Biol. Chem.* **276,** 33930–33937
6. Urbina, J. A., Moreno, B., Vierkotter, S., Oldfield, E., Payares, G., Sanoja, C., Bailey, B. N., Yan, W., Scott, D. A., Moreno, S. N. J., and Docampo, R. (1999) *J. Biol. Chem.* **274,** 33609–33615
7. Garzoni, L. R., Caldera, A., Meirelles, M. N., de Castro, S. L., Docampo, R., Meints, G. A., Oldfield, E., and Urbina, J. A. (2004) *Int. J. Antimicrob. Agents* **23,** 273–285
8. Garzoni, L. R., Waghabi, M. C., Baptista, M. M., de Castro, S. L., Meirelles, M. N., Britto, C. C., Docampo, R., Oldfield, E., and Urbina, J. A. (2004) *Int. J. Antimicrob. Agents* **23,** 286–290
9. Bouzahzah, B., Jelicks, L. A., Morris, S. A., Weiss, L. M., and Tanowitz, H. B. (2005) *Parasitol. Res.* **96,** 184–187
10. Ohnuma, S.-i., Hirooka, K., Tsuruoka, N., Yano, M., Ohto, C., Nakane, H., and Nishino, T. (1998) *J. Biol. Chem.* **273,** 26705–26713
11. Montalvetti, A., Fernandez, A., Sanders, J. M., Ghosh, S., Van Brussel, E., Oldfield, E., and Docampo, R. (2003) *J. Biol. Chem.* **278,** 17075–17083
12. Ellis, J. E., Setchell, K. D. R., and Kaneshiro, E. S. (1994) *Mol. Biochem.*

Parasitol. **65,** 213–224
13. Ranganathan, G., and Mukkada, A. J. (1995) *Int. J. Parasitol.* **25,** 279–284
14. Rassam, M. B., Shanshal, M., and Gargees, G. S. (1988) *Mol. Biochem. Parasitol.* **29,** 61–64
15. Clarkson, A. B., Bienen, E. J., Pollakis, G., and Grady, R. W. (1989) *J. Biol. Chem.* **264,** 17770–17776
16. Löw, P., Dallner, G., Mayor, S., Cohen, S., Chait, B. T., and Menon, A. K. (1991) *J. Biol. Chem.* **266,** 19250–19257
17. Kusel, J. P., and Weber, M. M. (1965) *Biochim. Biophys. Acta* **98,** 632–639
18. Vakirtzi-Lemonias, V. C., Kidder, G. W., and Dewey, V. C. (1963) *Comp. Biochem. Physiol.* **8,** 133–136
19. Michels, P.A., Moyersoen, J., Krazy, H., Galland, N., Herman, M., and Hannaert, V. (2005) *Mol. Membr. Biol.* **22,** 133–145
20. Okamoto, T., Fukui, K., Nakamoto, M., Kishi, T., Okishio, T., Yamagami, T., Kanamori, N., Kishi, H., and Hiraoka, E. (1985) *J. Chromatogr.* **342,** 35–46
21. Furuya, T., Kashuba, C., Docampo, R., and Moreno, S. N. (2000) *J. Biol. Chem.*, **275,** 6428–6438
22. Bone, G. J., and Steinert, M. (1956) *Nature* **178,** 308–309
23. Gerez de Burgos, N. M., Burgos, C., Blanco, A., Paulone, I., and Segura, E. L. (1976) *Acta Physiol. Lat. Am.* **26,** 10–19
24. Hall, T. A. (1999) *Nucl. Acids Symp. Ser.* **41,** 95–98
25. Altschul, S. F., Gish, W., Miller, W., Myers, E. W., and Lipman, D. J. (1990) *J. Mol. Biol.* **215,** 403–410
26. Kyte, J., and Doolittle, R. F. (1982) *J. Mol. Biol.* **157,** 105–132
27. Bendtsen, J. D., Nielsen, H., von Heijne, G., and Brunak, S. (2004) *J. Mol. Biol.* **340,** 783–795
28. Hanke, J., Sanchez, D. O., Henriksson, J., Åslund, L. C., Pettersson, U., Frasch, A. C. C., and Hoheisel, J. (1996) *BioTechniques* **21,** 686–693
29. Dretzen, G., Bellard, M., Sassone-Corsi, P., and Chambon, P. (1981) *Anal. Biochem.* **112,** 295–298
30. Búa, J., Garcia, G. A., Galindo, M., Galanti, N., and Ruiz, A. M. (1999) *Medicina* (*B Aires*) **59,** Suppl. 2, 11–17
31. Bradford, M. M. (1976) *Anal. Biochem.* **72,** 248–254
32. Koyama, T., Fujii, H., and Ogura, K. (1985) *Methods Enzymol.* **110,** 153–155
33. Okada, K., Minehira, M., Zhu, X., Suzuki, K., Nakagawa, T., Matsuda, H., and Kawamukai, M. (1997) *J. Bacteriol.* **179,** 3058–3060
34. Okada, K., Kainou, T., Tanaka, K., Nakagawa, T., Matsuda, H., and Kawamukai, M. (1998) *Eur. J. Biochem.* **255,** 52–59
35. Rohloff, P., Montalvetti, A., and Docampo, R. (2004) *J. Biol. Chem.* **279,** 52270–52281
36. Porcel, B. M., Tran, A. N., Tammi, M., Nyarady, Z., Rydaker, M., Urmenyi, T. P., Rondinelli, E., Pettersson, U., Andersson, B., and Aslund, L. (2000) *Genome Res.* **10,** 1103–1107
37. Yamauchi, K. (1991) *Nucleic Acids Res.* **19,** 2715–2720
38. Liang, P.-H., Ko, T.-P., and Wang, A. H.-J. (2002) *Eur. J. Biochem.* **269,** 3339–3354
39. Koyama, T. (1999) *Biosci. Biotechnol. Biochem.* **63,** 1671–1676
40. Chen, A., Kroon, P. A., Poulter, C. D. (1994) *Prot. Sci.* **3,** 600–607
41. Jun, L., Saiki, R., Tatsumi, K., Nakagawa, T., and Kawamukai, M. (2004) *Plant Cell Physiol.* **45,** 1882–1888
42. Hirooka, K., Bamba, T., Fukusaki, E., and Kobayashi, A. (2003) *Biochem. J.* **370,** 679–686
43. Alvarez, F., Robello, C., and Vignali, M. (1994) *Mol. Biol. Evol.* **11,** 790–802
44. Asai, K., Fujisaki, S., Nishimura, Y., Nishino, T., Okada, K., Nakagawa, T., Kawamukai, M., and Matsuda, H. (1994) *Biochem. Biophys. Res. Commun.* **202,** 340–345
45. Parsons, M. (2004) *Mol. Microbiol.* **53,** 717–724
46. Purdue, P. E., and Lazarow, P. B. (2001) *Annu. Rev. Cell Dev. Biol.* **17,** 701–752
47. Thompson, S. L., and Krisans, S. K. (1990) *J. Biol. Chem.* **265,** 5731–5735
48. Olivier, L. M., and Krisans, S. K. (2000) *Biochim. Biophys. Acta* **1529,** 89–102
49. Keller, G. A., Barton, M. C., Shapiro, D. J., and Singer, S. J. (1985) *Proc. Natl. Acad. Sci. U. S. A.* **82,** 770–774
50. Stamellos, K. D., Shackelford, J. E., Tanaka, R. D., and Krisans, S. K. (1992) *J. Biol. Chem.* **267,** 5560–5568
51. Krisans, S. K., Ericsson, J., Edwards, P. A., and Keller, G. A. (1994) *J. Biol. Chem.* **269,** 14165–14169
52. Tekle, M., Bentinger, M., Nordman, T., Appelkvist, E.-L., Chojnacki, T., and Olsson, J. M. (2002) *Biochem. Biophys. Res. Commun.* **291,** 1128–1133
53. Concepcion, J. L., Gonzalez-Pacanowska, D., and Urbina, J. A. (1998) *Arch. Biochem. Biophys.* **352,** 114–120
54. Pena-Diaz, J., Montalvetti, A., Flores, C. L., Constan, A., Hurtado-Guerrero, R., De Souza, W., Gancedo, C., Ruiz-Perez, L. M., and Gonzalez-Pacanowska, D. (2004) *Mol. Biol. Cell* **15,** 1356–1363
55. Bringaud, F., Baltz, D., and Baltz, T. (1998) *Proc. Natl. Acad. Sci. U. S. A.* **95,** 7963–7968
56. Acosta, H., Dubuordieu, M., Quiñones, W., Cáceres, A., Bringaud, F., and Concepción, J. L. (2004) *Comp. Biochem. Physiol. B* **138,** 347–356
57. Teclebrhan, H., Olsson, J., Swiezewska, E., and Dallner, G. (1993) *J. Biol. Chem.* **268,** 23081–23086
58. Swiezewaska, E., Dallner, G., Andersson, B., and Ernster, L. (1993) *J. Biol. Chem.* **268,** 1494–1499
59. Sagami, H., Ogura, K., and Seto, S. (1977) *Biochemistry* **16,** 4616–4622
60. Okada, K., Kamiya, Y., Zhu, X., Suzuki, K., Tanaka, K., Nakagawa, T., Matsuda, H., and Kawamukai, M. (1997) *J. Bacteriol.* **179,** 5992–5998
61. Zhang, Y. W., Koyama, T., and Ogura, K. (1997) *J. Bacteriol.* **179,** 1417–1419
62. Saiki, R., Nagata, A., Uchida, N., Kainou, T., Matsuda, H., and Kawamukai, M. (2003) *Eur. J. Biochem.* **270,** 4113–4121
63. Saiki, R., Nagata, A., Kainou, T., Matsuda, H., and Kawamukai, M. (2005) *FEBS J.* **272,** 5606–5622
64. Turunen, M., Olsson, J., and Dallner, G. (2004) *Biochim. Biophys. Acta* **1660,** 171–199
65. Ellis, J. E. (1994) *Parasitol. Today* **10,** 296–301
66. Kawamukai, M. (2002) *J. Biosci. Bioeng.* **94,** 511–517
67. Szajnman, S. H., Montalvetti, A., Wang, Y., Docampo, R., and Rodriguez, J. B. (2003) *Bioorg. Med. Chem. Lett.* **13,** 3231–3235